

SQAD: Automatic Smartphone Camera Quality Assessment and Benchmarking – Supplementary Material –

Zilin Fang¹, Andrey Ignatov², Eduard Zamfir³, Radu Timofte^{2,3}
¹National University of Singapore, ²ETH Zurich, ³University of Wurzburg

1. Dataset Overview

Here we provide the complete quality factor measurement results of our SQAD dataset in Tab. 5. Reported factor results are the measurement average of 9 images. Specially, in PSF we apply four horizontal and four vertical patterns to compute the average. The illuminance level for noise and dynamic range measurement in the dark room is nearly 0 lux before applying the OLED screen, while for the remaining patterns the illuminance level is approximately 1000 lux.

2. Methods and Theorems

Resolution Measurement. We summarize the algorithm applied to evaluate the resolution in Algorithm 1.

Algorithm 1: Resolution from wedge pattern

Result: *resol* in LW/PH

Pattern range initialization: $L = [L_{min}, L_{max}]$;

1. Detect whole pattern with thresholding;

2. Indices mark (black line) finding: $IdxBars$;

for i **to** numbers of contours **do**

if $Ratio_{W/H}(i) \in Range$ **then**
 | $IdxBars \leftarrow BoundingBox(i)$

end

end

sort($IdxBars$) according to y coordinate;

3. Detect wedge region: filtering + edge detection;

4. Initialize every wedge component's center: $arrC$;

5. Track centers with interval updates;

 Interval $interv = \text{mean}(max_{arrC} - min_{arrC})$;

for $loc \leftarrow 1$ **to** H_{wedge} **do**

foreach element e of the centers **do** $arrC(e) \leftarrow$

 FindNewPeak(loc);

 update $interv$ with new centers;

if $MinPeakProminence(loc) < 2$ **then**

break;

end

end

$resol = \text{transformed}(loc)$ with $IdxBars$ and L ;

CIEDE2000 color difference formula. We simply refer to the formula from [3] (as in Eq. (3)) in where five important corrections are included to solve perceptual uniformity:

$$\Delta E_{00}^{12} = \sqrt{\left(\frac{\Delta L'}{k_L S_L}\right)^2 + \left(\frac{\Delta C'}{k_C S_C}\right)^2 + \left(\frac{\Delta H'}{k_H S_H}\right)^2 + R_T \frac{\Delta C'}{k_C S_C} \frac{\Delta H'}{k_H S_H}} \quad (3)$$

with parametric weighting factors k_L , k_C and k_H , the chroma difference $\Delta C'$, the hue difference $\Delta H'$, and $\Delta L = L_2 - L_1$. All the other terms are computed from two CIELAB color values $\{L_1, a_1, b_1\}$ and $\{L_2, a_2, b_2\}$. More calculation details are provided in their original paper [3].

Dynamic Range Measurement. The scene SNR is calculated using Eq. (4) and Eq. (5), and is determined by scaling the ISO SNR with a factor. $\sigma_{f_{stop}}$ in Eq. (4) is the scene noise in logarithmic units of f-stops:

$$\begin{aligned} \sigma_{f_{stop}} &= \frac{\sigma}{d\text{pixel}/df_{stop}} = \frac{\sigma}{d\text{pixel}/d\log_2 L} \\ &= \frac{\sigma}{\ln(2) * L * d\text{pixel}/dL} \cong \frac{\sigma}{L * d\text{pixel}/dL} \end{aligned} \quad (4)$$

where scene luminance L (or exposure) is the signal level of the scene, and there is a relationship between different units: 1 f-stop = 6.02 dB = $\log_2 L$. Then, the scene noise and SNR can be expressed by Eq. (5). It finally leads to $SNR_{scene} = \ln(2) SNR_{ISO}$.

$$\begin{aligned} \sigma_{scene} &= \frac{\sigma}{d\text{pixel}/dL} \cong \sigma_{f_{stop}} * L \\ SNR_{scene} &= \frac{L}{\sigma_{scene}} = \frac{1}{\sigma_{f_{stop}}} \end{aligned} \quad (5)$$

To enable a representation directly from signals and noise in pixels, [1] further introduces scene-referenced noise and SNR in Eq. (6). The equivalence between SNR_{scene} and SNR_{ref} establishes a connection between pixel noise and scene noise which cannot be measured directly. It is the calculation basis for [1].

$$\begin{aligned} \sigma_{ref} &= \frac{\sigma}{d\text{pixel}/dL} \cdot \frac{\text{pixel}}{L} \\ SNR_{ref} &= \frac{\text{pixel}}{\sigma_{ref}} = \frac{L}{\sigma/(d\text{pixel}/dL)} = SNR_{scene} \end{aligned} \quad (6)$$

Table 5: *Overview of our data collection.* Our dataset comprises of 29 different devices reflects the development of smartphone photography over the last decades. Note, for some devices definite image sensor models were not available (-).

| No. | Name | Device Specifications | | | Sensor Quality Factors | | | | | |
|-----|------------------------------|-----------------------|------------|--------------------|------------------------|----------------|---------|---------------|-------|---------------------|
| | | Year | Image Size | Sensor | Resolution | Color Accuracy | Noise | Dynamic Range | PSF | Aliasing |
| 1 | ASUS Z00AD | 2015 | 4096*3072 | T4K37 | 8.57 | 947.94 | 3.7912 | 6.6438 | 68.3 | 0.0699 |
| 2 | CANON EOS70D | 2013 | 3648*2432 | - | 29.22 | 745.74 | 1.8789 | 9.6336 | 17.8 | 0 |
| 3 | Google Pixel 2 | 2017 | 4032*3024 | IMX362 | 13.77 | 684.54 | 2.6599 | 7.6404 | 27.5 | 0.0746 |
| 4 | Google Pixel 6 | 2021 | 4080*3072 | ISOCELL GN1 | 11.95 | 637.27 | 2.5658 | 7.6404 | 39.5 | 0.0965 |
| 5 | HTC DesireEye | 2014 | 4208*2368 | IMX214 | 12.59 | 915.51 | 4.064 | 6.3117 | 59.6 | 0.0717 |
| 6 | HTC One (M7) | 2012 | 2688*1520 | VD6869 | 5.7 | 952.16 | 6.2865 | 5.9795 | 54.5 | 0.2931 |
| 7 | HTC One X+ | 2012 | 3264*1840 | - | 7.48 | 902.7 | 2.6295 | 6.3117 | 56.3 | 0.0996 |
| 8 | HUAWEI P8Lite | 2015 | 4160*3120 | IMX214 | 10.62 | 474.78 | 3.4722 | 7.3082 | 62.4 | 0.077 |
| 9 | HUAWEI P30Pro | 2019 | 3648*2736 | IMX600y | 26.71 | 706.83 | 1.4529 | 8.637 | 22.5 | 0.0841 ² |
| 10 | LG G3 | 2014 | 4160*3120 | IMX135 | 16.66 | 902.93 | 12.0148 | 7.6404 | 70.3 | 0.07 |
| 11 | Nexus 6 | 2014 | 4160*3120 | IMX214 | 11.1 | 531.27 | 1.7157 | 7.6404 | 64.8 | 0.086 |
| 12 | Nokia asha300 | 2011 | 2592*1944 | - | 7.88 | 897.55 | 5.2513 | 6.976 | 51.6 | 0.0827 |
| 13 | Nokia N79 | 2008 | 2592*1944 | - | 8.56 | 795.29 | 4.0134 | 6.976 | 65.7 | 0.122 |
| 14 | OPPO A92S | 2020 | 4000*3000 | IMX586 | 9.57 | 905.39 | 1.8599 | 6.6438 | 51.5 | 0.0827 |
| 15 | Realme X7Pro | 2020 | 4608*3456 | IMX686 | 10.45 | 736.32 | 2.6861 | 6.6438 | 50.0 | 0 |
| 16 | Samsung GalaxyNote20 Ultra5G | 2020 | 4000*3000 | ISOCELL HM1 | 11.74 | 736.91 | 1.7211 | 7.3082 | 52.5 | 0.0908 |
| 17 | Samsung Galaxy S4 | 2013 | 4128*2322 | IMX091PQ | 13.33 | 838.65 | 2.0311 | 6.976 | 52.7 | 0.0734 |
| 18 | Samsung Galaxy S5 | 2014 | 5312*2988 | ISOCELL 2P2 | 14.33 | 806.69 | 4.624 | 6.976 | 48.0 | 0.0567 |
| 19 | Samsung Galaxy S6 edge | 2015 | 5312*2988 | IMX240/ISOCELL 2P2 | 12.9 | 863.93 | 3.1192 | 6.976 | 51.0 | 0.0624 |
| 20 | Samsung Galaxy S10 | 2020 | 4032*2268 | ISOCELL 2L4 | 18.64 | 712 | 2.9899 | 7.3082 | 24.4 | 0 |
| 21 | Samsung GT-I9100 | 2011 | 3264*2448 | ISOCELL 3H2 | 8.19 | 931.12 | 2.5423 | 6.6438 | 79.0 | 0.0925 |
| 22 | Samsung GT-I9300 | 2012 | 3264*2448 | ISOCELL 3H2 | 9.64 | 876.85 | 3.3558 | 7.3082 | 64.5 | 0.0944 |
| 23 | Sony Ericsson T630 | 2003 | 640*480 | - | 2.15 | 862.57 | 10.1393 | 5.9795 | 168.7 | 0.3904 |
| 24 | Sony Ericsson vivaz | 2010 | 3264*1836 | - | 10.56 | 984.92 | 1.8174 | 6.976 | 48.4 | 0.1082 |
| 25 | Sony Ericsson W810 | 2006 | 1632*1224 | - | 6.14 | 868.28 | 2.6588 | 6.3117 | 138.8 | 0.2865 |
| 26 | Sony st2li | 2012 | 2048*1536 | - | 3.33 | 757.66 | 2.884 | 6.976 | 87.8 | 0.1616 |
| 27 | Sony Xperia XA1Ultra | 2017 | 5520*4144 | IMX300 | 11.06 | 658.05 | 1.5321 | 7.6404 | 58.0 | 0 |
| 28 | Sony Xperia Z5Compact | 2015 | 3840*2160 | IMX300 | 13.41 | 773.8 | 3.6219 | 5.3151 | 46.9 | 0.0708 |
| 29 | Sony Xperia Z | 2013 | 3920*2204 | IMX135 | 9.96 | 950.31 | 2.2291 | 5.9795 | 48.3 | 0.0692 |

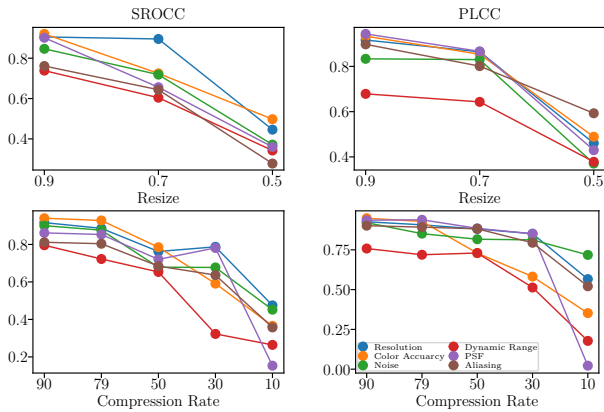


Figure 6: *Results on image quality degradation for ResNet50 [2] model.* We include JPEG lossy compression and image resizing as degradations. Results are multi-crop (16×) predictions.

We apply the above equations in DR measurement process and the results are expressed in SNR with f-stop units. Considered indicators exhibit considerable independence from image signal processing and flare light-induced fogging, which is excellent for real-world camera performance.

3. Visualizations

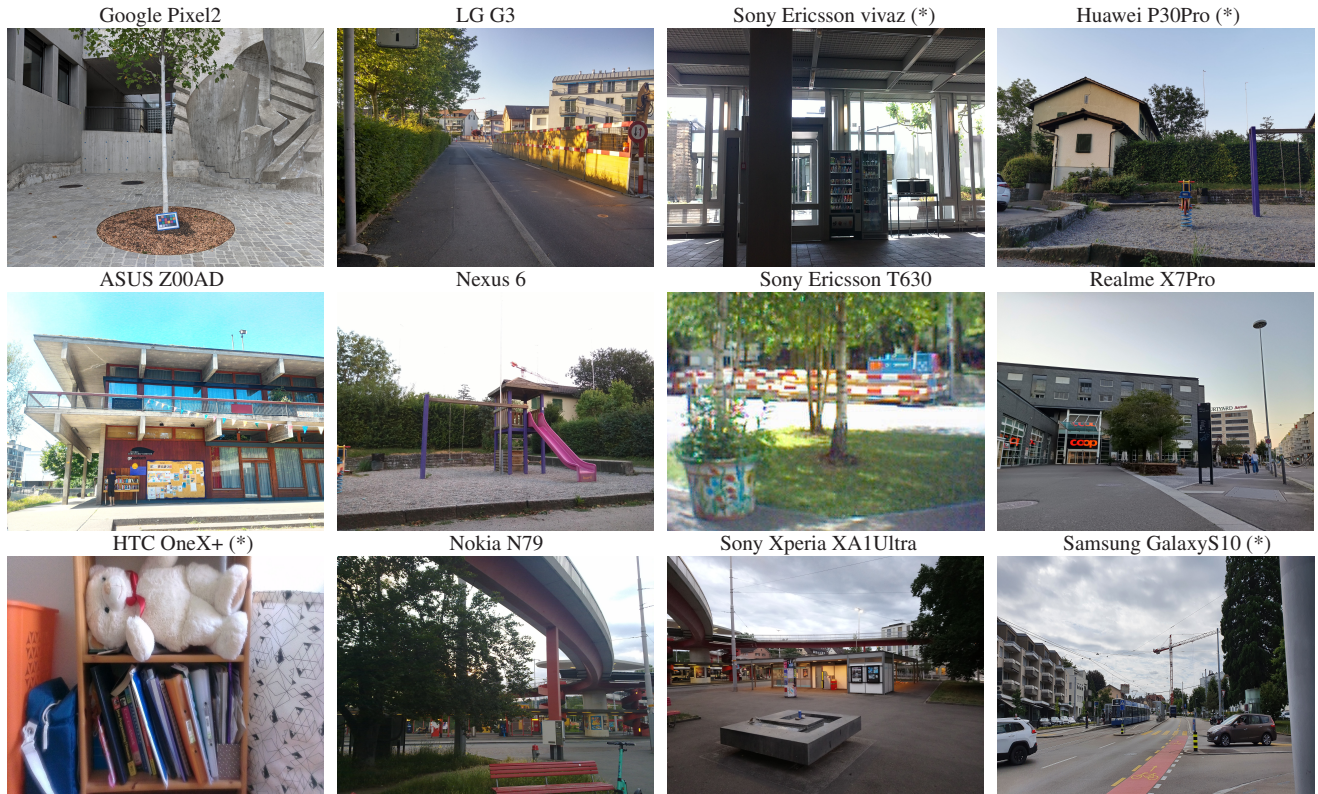
We provide examples captured with different cameras from our SQUAD dataset in Fig. 7.

In addition to the ablations in the main text, we also

illustrate a regression analysis for various image degradation settings in Fig. 6. Under the same compression rate or resize ratio with ResNet50 backbone, the trained model achieves SROCC/PLCC scores > 0.6 on the test set if distortions are not severe, which proves the ability to tolerate some image degradations. In practice, impairment levels may vary across different photos on the Internet, and we will investigate this further in future works.

References

- [1] Imatest: Solutions on image quality factors. <https://www.imatest.com/solutions/iqfactors/>. 1
- [2] Kaiming He, Xiangyu Zhang, Shaoqing Ren, and Jian Sun. Deep residual learning for image recognition. In *Proceedings of the IEEE conference on computer vision and pattern recognition*, pages 770–778, 2016. 2
- [3] Gaurav Sharma, Wencheng Wu, and Edul N Dalal. The ciede2000 color-difference formula: Implementation notes, supplementary test data, and mathematical observations. *Color Research & Application: Endorsed by Inter-Society Color Council, The Colour Group (Great Britain), Canadian Society for Color, Color Science Association of Japan, Dutch Society for the Study of Color, The Swedish Colour Centre Foundation, Colour Society of Australia, Centre Français de la Couleur*, 30(1):21–30, 2005. 1



(a) Images for different scenarios.



(b) Images for the same scenario.

Figure 7: Examples images taken from SQAD dataset. Images taken with devices marked by asterisks (*) are resized for visualization. The image taken with Sony Ericsson T630 portrays the same scene as in Fig. 2 of the main text.